Pergamon

PII: S0008-6223(98)00026-8

RAMAN STUDIES ON SINGLE WALLED CARBON NANOTUBES PRODUCED BY THE ELECTRIC ARC TECHNIQUE

M. Lamy de la Chapelle,[a,*] S. Lefrant,[a] C. Journet,[b] W. Maser,[b] P. Bernier[b] and A. Loiseau[c]

[a]IMN-Univ. Nantes, BP 32229, 44322 Nantes Cedex 3, France
[b]GDPC-Univ. Montpellier II, 34095 Montpellier Cedex 5, France
[c]Lab. Phys. Solide, ONERA, BP 72, 92322 Châtillon Cedex, France

Abstract—Carbon single walled nanotubes (SWNTs) have been produced in high yields using the electric arc technique. TEM studies show that the SWNTs have a narrow diameter distribution around an average value of 1.3 nm. In this paper, we focus on the characterization of these samples by high resolution Raman spectroscopy (HRRS). The presence of large amounts of SWNTs in the samples induces a very rich structure in the Raman spectra, typical for this class of carbonaceous material. Armchair tubes with (8,8) to (12,12) geometry can be detected, in agreement with the narrow diameter distribution observed by TEM measurements. The ability of HRRS as a highly sensitive fingerprint technique in identifying SWNTs with different diameters and geometries is discussed. © 1998 Elsevier Science Ltd. All rights reserved.

Key Words—A. Carbon nanotubes, C. Raman spectroscopy.

1. INTRODUCTION

Since their discovery in 1991 [1], carbon nanotubes (CNTs) have been presented as very promising materials both for their electronic and mechanical properties. Before last year, the main obstacle to their study was the difficulty of producing samples in large amounts. But recently, Thess *et al.* [2] and Journet *et al.* [3] have proposed new methods using double laser ablation of a carbon–nickel–cobalt mixture and electric arc techniques, respectively, to obtain a yield of more than 70% of single walled nanotubes (SWNTs). So from samples produced with the latter method, we present here a Raman study of SWNTs, and such yields allow us to suggest that the different Raman spectra shown are characteristic of SWNTs. Moreover, some features reveal a tube diameter distribution or different chirality. These observations show the real importance of Raman spectroscopy to characterize both qualitatively and quantitatively our samples with a non-destructive method.

2. SYNTHESIS

Single walled carbon nanotubes were produced by creating an electric arc discharge between two graphite rods. The anode was drilled and filled with a mixture of nickel and yttrium used as catalysts. The synthesis was performed in a water-cooled chamber first evacuated and then filled with a static pressure of 660 mbar of helium. A current of 100 A was applied and a voltage of about 35 V was maintained constantly by continuously translating the anode towards the cathode. More details on this synthesis can be found in Ref. [3]. After the synthesis, two kinds of extracted products were characterized: the soot on reactor walls and the "collaret" around the deposit on the cathode.

3. EXPERIMENTAL RESULTS

Raman experiments have been performed with a Jobin Yvon T64000 spectrophotometer in ambient air and temperature. Spectra have been recorded using three different wavelengths: 457.9 nm (blue), 514.5 nm (green) and 676.4 nm (red). In Figs 1 and 2, only one spectrum is presented for each wavelength. In Figs 3 and 4, we present Raman spectra obtained with the blue and green lines, 2 and 3,
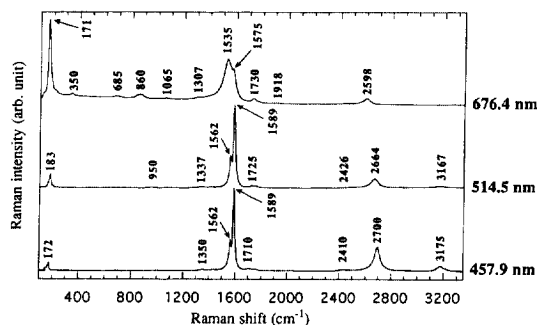

Fig. 1. Raman spectra of single walled carbon nanotubes. Excitation: 457.9, 514.5 and 676.4 nm.

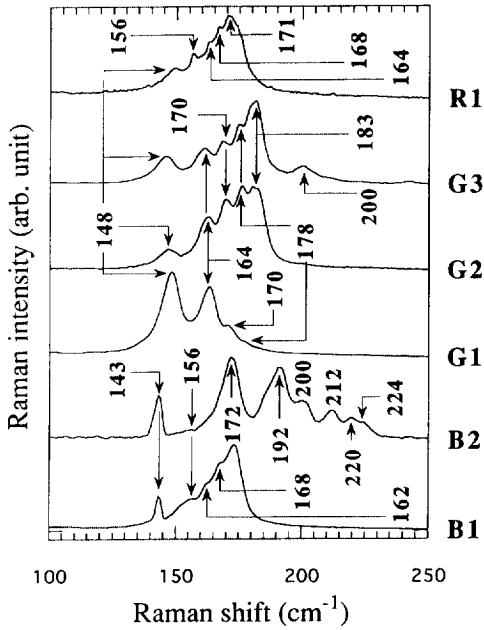*Corresponding author. Fax: +33 240 37 39 91; e-mail: lamy@cnrs-imn.fr

Fig. 2. Details of the low frequency bands (140–200 cm^{-1}). Excitation: 457.9, 514.5 and 676.4 nm.
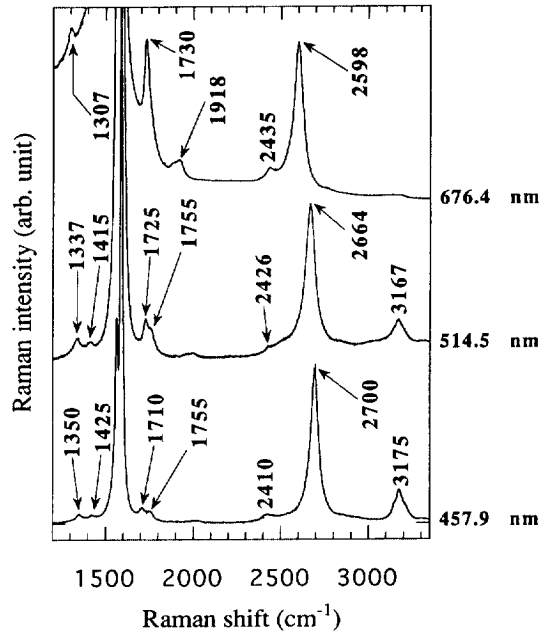

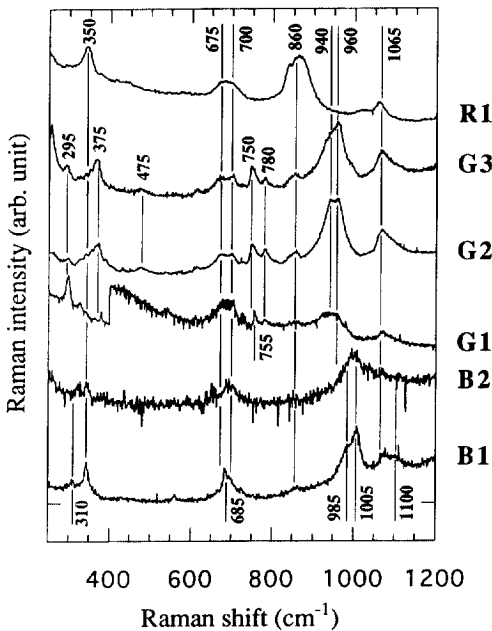Fig. 4. Second order Raman spectra. Excitation: 457.9, 514.5 and 676.4 nm.

Fig. 3. Details of the intermediate frequency range (250–1200 cm^{-1}). Excitation: 457.9, 514.5 and 676.4 nm.

respectively, issued from different spots of the sample. In this case, the label of each spectrum indicates by the first letter the laser excitation line (B = blue, G = green and R = red) and the number indicates that the spectrum has been recorded on different spots of the sample. As shown by Figs 1 and 4, different groups of bands can easily be observed on all spectra whatever the wavelength used.

First, between 1500 and 1600 cm^{-1}, we can distin-

guish at least four components near 1589, 1560, 1550 and 1530 cm^{-1} on spectra recorded with the blue and green light excitation. The existence of these last components, which only appeared as shoulders with the other excitations, is confirmed by the inversion of their relative intensity compared to what is obtained with the red line excitation, since the more intense band is now located at 1535 cm^{-1} with a second peak near 1575 cm^{-1}. These features can be explained by the tube structure considered as enroled graphitic layers. Indeed, graphene sheets give one E_{2g2} mode at 1582 cm^{-1}. But the introduction of some curvature removes the degeneracy of this mode and induces change from a 2-D to a 3-D symmetry. So, one A_g mode is upshifted near 1590 cm^{-1} whereas the other one, E_{1g}, is downshifted. This is in agreement with calculations performed by Bacsa *et al.* [4] who predict a frequency dependence of this mode as a function of the tube diameter, in the range 1580 and 1520 cm^{-1}, since this frequency depends on the tube diameter. In this region, other modes have also been calculated [5,6] and can also contribute to the Raman band intensities. As a consequence, the assignment of each contribution is not straightforward. Otherwise, the enhancement of the lower frequency components is explained by resonance effects, since the laser energy is close to that of transitions between two electronic levels. Since resonance effects can be associated with either a selective excitation of nanotubes of particular diameter or a selective excitation of nanotubes with a specific configuration related to its chirality (armchair, zigzag or chiral tube).

Second, in the low frequency range between 140 and 240 cm^{-1}, the good frequency resolution (less

than 3 cm^{-1}) allows us to resolve several close peaks shown in Fig. 3. Raman spectra obtained with the blue excitation show several bands (nine): 156, 162, 168, 172, 192, 200, 212, 220, 224 cm^{-1} (the narrow line at 143 cm^{-1} is a laser one); six Raman bands are recorded for the green line excitation: 148, 164, 170, 178, 183, 200 cm^{-1}; and five for the red line excitation: 148, 156, 164, 168, 171 cm^{-1}. These observations show that the position of each band is independent of the experimental conditions, whereas the relative intensities depend both on the laser spot and on the wavelength used. The first point has to be associated with the breathing mode A_g of the tube as calculated by Rao et al. [6]. Indeed, we expect that the frequency of this mode, located between 130 and 260 cm^{-1}, depends on the tube diameter, since a higher diameter gives lower frequency. So we suggest that one band corresponds to one diameter. Then each relative intensity provides the proportion of a particular diameter in the studied area and the whole group of bands reflects the diameter distribution in this same area. The difference observed on Raman spectra recorded with the same wavelength puts in evidence the sample inhomogeneity. For example, although the spectrum G1 presents a large proportion of large diameter tubes, the distribution can completely change in another area of the same sample as shown in spectrum G2. A better understanding of these features and a clear assignment of each band will lead to a real quantitative characterization of our samples. Another behaviour is observed when changing excitation wavelength. It appears that the overall intensity of this group of bands is greatly enhanced with the red line and becomes more intense in the Raman spectrum (Fig. 1). Moreover, the features presented in Fig. 3 show that new bands appear at 156 cm^{-1} (B1, B2, R1) or 192 cm^{-1} (B2), whereas some are no longer observed, such as the band at 183 cm^{-1} (G2, G3). In this case, in contrary to the first group of bands, the low frequency bands give evidence of resonance effects not only for the red light excitation but also for the blue line. These results seem to eliminate the first given origin for resonance effects. Indeed, if only one diameter is excited, then only one band is enhanced. But we can always see a diameter distribution presented previously whatever the wavelength used. So we can reasonably think that all spectra are in fact the superposition of the response of several tube diameters.

Third, the second order Raman spectra exhibit strong peaks at 2700, 2664 and 2598 cm^{-1} for, respectively, blue, green and red excitations. In graphite, this band, called the D* line, is the overtone of a non-centre optical phonon branch near the points M and K of the edge of the Brillouin zone which also gives the D line assigned to disordered graphitic structure. This D line is also observable but weakly on our spectra at 1350, 1337 and 1307 cm^{-1} with blue, green and red light, respectively. We can attribute it to the disorder induced by the tube curvature but also to the small amount of glassy carbon produced simultaneously. On the graphite spectrum, the D* line presents two contributions from the M and K points, respectively, on the higher and lower frequency sides. In our case, this band is perfectly symmetric which suggests that it is only dominated by the K point contribution. It can also be noted that the frequency and intensity decrease with the laser energy. The first and second observations are in agreement with the results so far obtained from multi-walled carbon nanotubes (MWNTs) and are attributed to a dispersion effect with different resonance enhancements of the contribution from regions near the K and M points [7]. But concerning intensity, the behaviour is the opposite. Indeed, the intensity increases with laser energy for SWNTs, whereas it increases with wavelength for MWNTs as for disordered graphitic structure due to an enhancement of the G line from the $\pi-\pi^*$ transition with low wavelength. This suggests that the electronic structure of SWNTs is not similar to that of MWNTs and that the superposition of several layers induces changes in each.

Several weak features are also observable, significantly in the range of frequency 250–1200 cm^{-1}. All these peaks can be classified into two kinds: those which are always observable and those specific to one wavelength. The first category is composed of four groups of bands: 290–400, 860, 675–700 and 1060–1100 cm^{-1}. Between 290 and 400 cm^{-1}, we can see the overtones of the low frequency group of bands (140–240 cm^{-1}). Indeed, these peaks always present the same structure and frequencies very close to twice the values of low frequency bands. The other groups present resonance behaviour such as the 860 cm^{-1} band which is an E_{2g} symmetry mode [6] and whose intensity increases with the wavelength. Otherwise, for the two latter groups, the relative intensities of bands change from a laser line to the other. Between 675 and 700 cm^{-1}, whereas this group can be seen as a wide band with red excitation, two peaks dominate at 675 and 700 cm^{-1} with the green light and with the blue one; it exhibits an asymmetric profile on the high frequency side with a maximum at 685 cm^{-1}. The 1060–1100 cm^{-1} group shows the same behaviour: one peak at 1065 cm^{-1} with red light, an asymmetric one with green light and two peaks at 1070 and 1100 cm^{-1} with blue light. For the second category, one remarkable peak is that located on the Raman spectra recorded with green light excitation between 750 and 780 cm^{-1}, which presents an asymmetric profile on the high frequency side. Indeed, it gives evidence of the existence of armchair tubes in our sample since calculations show that only this kind of tube has vibrational modes predicted in this frequency range [5,6]. Moreover, in this region, the calculated mode is an E_{1g} one whose frequency increases with the tube diameter and goes from 750 to 770 cm^{-1} from (6/6) to (12/12) tubes.

So, the asymmetry can be explained as the superposition of several bands and then reflects a diameter distribution as for the low frequency group of bands. This is confirmed by the evolution of this peak on the spectra G1, G2 and G3. If we compare the low frequency bands of these three spectra, we can see that the proportion of the lowest diameters increases from G1 to G3. At the same time, the maximum of the peak is upshifted from 755 to 750 cm^{-1} between G1 and G2 and gets narrower on G3, which well reflects the same evolution as the low frequency bands. Therefore, we can assert that our samples contain armchair tubes from (6/6) to (12/12). On the same spectra, we can see a wide peak between 900 and 1000 cm^{-1}. Since its profile also changes with the diameter distribution, we can suggest that it is the superposition of several bands which are too close to be resolved. Even if we cannot give any assignment because no calculations predict modes in this frequency range [5,6], we can show that it shifts to higher frequency when the tube diameter is smaller in the area studied. Indeed, on G3 compared to G2, we can see a decrease of the lower frequency side near 940 cm^{-1} and the apparition of a shoulder near 980 cm^{-1}, a change which can be once again correlated to the evolution of the low frequency group of bands. A last feature is observable on spectra recorded with the blue line between 960 and 1020 cm^{-1}, which also seem to be constituted by several peaks, especially one at 985 cm^{-1} and another at 1005 cm^{-1}, whose origin is not known.

On all these observed modes, the assignment of only a few of them is well established, such as the E_{1g} mode near 750 cm^{-1}, the E_{2g} mode at 860 cm^{-1} and the overtones of the low frequency bands. All others either do not correspond to calculated modes such as those located between 900 and 1100 cm^{-1}, or do not evolve with the diameter distribution as given by calculations. So, at the present time, we cannot give a complete interpretation of these last features, even if we are able to see correlations. Moreover, except for the overtones, no mode gives the same response from one wavelength to another, due again to important resonance effects. The main change is the disappearance of the peaks between 750 and 780 cm^{-1} on spectra recorded with blue and red light excitation. Indeed, we have previously assigned these modes as originating from armchair tubes. These modes are not observed with blue and red light excitations, but the presence of a peak at 675–700 cm^{-1} could be a signature of zigzag tubes for which new resonance conditions are fulfilled. This

peak exclude chiral tubes for which no mode is calculated in this frequency region. But with blue and red excitation, we can observe several differences.

The second order spectra show weak features in addition to the D* line. First, near 1720 and 1420 cm^{-1}, we can observe a combination of modes between the E_{2g2} mode with the low frequency modes and its first overtone near 3170 cm^{-1}. For the 1918 and near 2420 cm^{-1}, no clear assignment is given so far.

4. CONCLUSION

In this paper, we have reported experimental Raman results on single walled nanotubes produced by the electric arc discharge, using different excitation wavelengths and investigating different spots on one samples. A distribution of diameters for the nanotubes is put into evidence by a strong dependence of some Raman modes as a function of excitation wavelength. According to previous calculations, we can infer that "armchair" tubes (6/6) to (12/12) are present, in agreement with high resolution TEM measurements. Specific resonance effects are shown for the different nanotubes. Raman scattering is used here as an efficient technique for a qualitative and quantitative characterization of SWNTs in a non-destructive way.

REFERENCES

1. Iijima, S., *Nature*, 1991, **354**, 56.
2. Thess, A., Lee, R., Nikolaev, P., Dai, H., Petit, P., Robert, J., Xu, C., Lee, Y. H., Kim, S. G., Rinzler, A. G., Colbert, D. T., Scuseria, G. E., Tomanek, D., Fischer, J. E. and Smalley, R. E., *Science*, 1996, **273**, 483.
3. Journet, C., Maser, W., Bernier, P., Loiseau, A., Lamy de la Chapelle, M., Lefrant, S., Lee, R. and Fischer, J., *Nature* (in press).
4. Bacsa, W. S., Ugarte, D., Châtelain, A. and de Heer, W., *Phys. Rev. B*, 1994, **50**(20), 15473.
5. Eklund, P. C., Holden, J. M. and Jishi, R. A., *Carbon*, 1995, **33**(7), 959.
6. Rao, A.M., Richter, E., Bandow, S., Chase, B., Eklund, P. C., Williams, K. A., Fang, S., Subbaswamy, K. R., Menon, M., Thess, A., Smalley, R. E., Dresselhaus, G. and Dresselhaus, M. S., *Science*, 1997, **275**, 187.
7. Kastner, J., Pichler, T., Kuzmany, H., Curran, S., Blau, W., Weldon, D. N., Dalemesiere, M., Draper, S. and Zandbergen, H., *Chem. Phys. Lett.*, 1994, **221**, 53.